Mid-latitude effects of "expanded" geomagnetic substorms: a case study

Veneta Guineva[1,*], *Irina* Despirak[2], *Rolf* Werner[1], *Rumiana* Bojilova[3], *Lyubomira* Raykova[1]

[1]Space Research and Technology Institute (SRTI), Bulgarian Academy of Sciences, Stara Zagora Department, Bulgaria
[2]Polar Geophysical Institute, Apatity, Russia
[3]National Institute of Geophysics, Geodesy and Geography (NIGGG), Bulgarian Academy of Sciences, Sofia, Bulgaria

Abstract. The goal of this work is to examine the effects of the "expanded" or "high-latitude" substorms at mid-latitudes. These substorms are generated at auroral latitudes and propagate up to geomagnetic latitudes above ~70° GMLat. They are usually observed during reccurent high-speed streams (HSS) from coronal holes. To identify the substorm activity, data from the networks IMAGE, SuperMAG and INTERMAGNET, and data from the all-sky cameras in Lovozero were used. To verify the interplanetary and geomagnetic conditions, data from the CDAWeb OMNI and from the WDC for geomagnetism at Kyoto were taken. We analyzed one substorm event on 20 February 2017 at ~18:40 UT, it developed during HSS, in non-storm conditions. Some features of mid-latitude positive bays (MPB) at the European and Asian stations, and in particular at the Scandinavian meridian have been studied: the bay sign conversion from negative to positive values, the longitudinal and latitudinal extent of the MPB. The central meridian of the substorm was determined.

1. Introduction

Substorms are a specific phenomenon, related to a number of processes in the magnetosphere and ionosphere, generalized by Akasofu [1]. Magnetospheric substorms are the reason for the main magnetic disturbances in the Earths magnetosphere. It is known that substorms are a typical phenomenon at auroral latitudes (~ 60°- ~ 71° MLAT) [2]. Although, according to the conditions in the solar wind and the magnetic activity, substorms can propagate to very high latitudes (above 70° MLAT) (>70° MLAT) (e.g. [3-5] as well as to spread to middle latitudes (~ 50° MLAT) [6]. It has to be noted, that substorms, appeared during different solar wind conditions, usually differ considerably from each other (eg., [7], [8], [9], [10]). Consequently, the substorms have been classified into different types, as: "limited" and "extended" [11], "localized" and "normal" [12], "substorms on the contracted oval" and "normal" [13], "polar" and "usually" [14], "high latitude" and "normal" [5], "extended" and "polar" [15].

*Corresponding author: v_guineva@yahoo.com

© The Authors, published by EDP Sciences. This is an open access article distributed under the terms of the Creative Commons Attribution License 4.0 (http://creativecommons.org/licenses/by/4.0/).

It should be noticed, that the midlatitude effects of substorms, by contrast to the ones at auroral latitudes, are expressed by positive bays in the X-component of the magnetic field at ground [16]. At first, this effect was associated with the low latitude return currents of the westward electrojet [17]. Later, the presence of positive bays was connected to the upward field-aligned currents [18]. The accepted theory at present is, that the midlatitude positive bays are the result of a current system, namely the Substorm Current Wedge (SCW) [19,16]. Therefore, taking into account the variety of substorms types, the positive bays development at middle latitudes during substorms can also have some peculiarities, depending on the different conditions. So, the midlatitude effects of different types of substorms should be investigated. In this work, we focused our efforts to estimate the specificity of midlatitude bays development during "expanded" or "high-latitude" substorms. The expanded substorms occur at auroral latitudes, and spread to very high latitudes, above ~70° GMLat. Two expanded substorms have been selected to be presented in detail: on 20 February 2017 and on 30 March 2013.

2. Data used

For the substorm identification and for the study of the substorms development, data from the magnetometer networks IMAGE, SuperMAG and INTERMAGNET, and data from the all-sky cameras in Apatity and in Barentsburg were used.

To verify the interplanetary and geomagnetic conditions, data from the CDAWeb OMNI (http://cdaweb.gsfc.nasa.gov/), from the catalog of large-scale solar wind phenomena (http://www.iki.rssi.ru/omni/) and from the WDC for geomagnetism at Kyoto (http://wdc.kugi.kyoto-u.ac.jp/index.html) were taken.

3. Interplanetary and geomagnetic conditions

One case of expanded substorm, the substorm at 18:40 UT on 17 February 2017 was considered. The interplanetary and geomagnetic conditions during the substorm are presented in Fig.1. From up to down the following quantities are drawn: the magnitude of the IMF vector, the IMF By component, the IMF Bz component, the velocity V, the dynamic pressure P, the PC index, the SYM/H index and the SML index. The boundaries of the structures in the solar wind are marked by rectangles. The dashed vertical line indicates the substorm onset.

From the left upper panel it is seen that during the time interval 16 – 21 February 2017 two consecutive structures in the solar wind were observed: CIR in front of a High-speed stream (HSS). The CIR begun at 7 UT on 16 February 2017 and lasted 24 hours. The HSS was observed from 7 UT on 17 February to 24 UT on 20 February 2017.

There was no magnetic storm developed, SYM/H was ~-18 nT. The considered substorm was registered during HSS in the solar wind. The SML index was ~ -800 nT. The behavior of the solar wind parameters before the substorm onset is presented in more detail in the right panel of Fig.1.

4. Substorm development

The substorm development at ~18:40 UT on 20 February 2017 is presented in Fig.2. In the upper panels the ground-based magnetic disturbances in the X (left upper panel) and Z (right upper panel) magnetic field components from 12 UT to 24 UT on 20.02.2017 by the IMAGE magnetometers chain (NAL-PPN) are shown. The substorm disturbances are marked by ellipses. The substorm onset was at auroral latitudes, 66°-68° GMLat (the region between

MAS-SOR stations) and the disturbances spread up to NAL station (76.6° GMLat), i.e., above 75° GMLat. The center of the westward electrojet was between the stations LYR and NAL (75.6° – 76.6° GMLat). So, this substorm was high-latitude, or expanded. From the X component variations it is seen, that the sign conversion latitude of the magnetic bays lays at about 60° GMLat (between the HAN and RAN stations). In the bottom panels, the substorm development by data of the Polar Geophysical Institute (PGI) is given. The left panels present the magnetic field components at Barentsburg (BAB) and Lovozero (LOZ) stations. It is seen that at these longitudes, the substorm is observed as at auroral latitudes (~64° GMLat), as well as at higher latitudes (above ~75° GMLat). The right bottom panels present the substorm development by aurora, measured in the 5577Å emission at LOZ. The substorm bulge expansion from South to North is clearly seen.

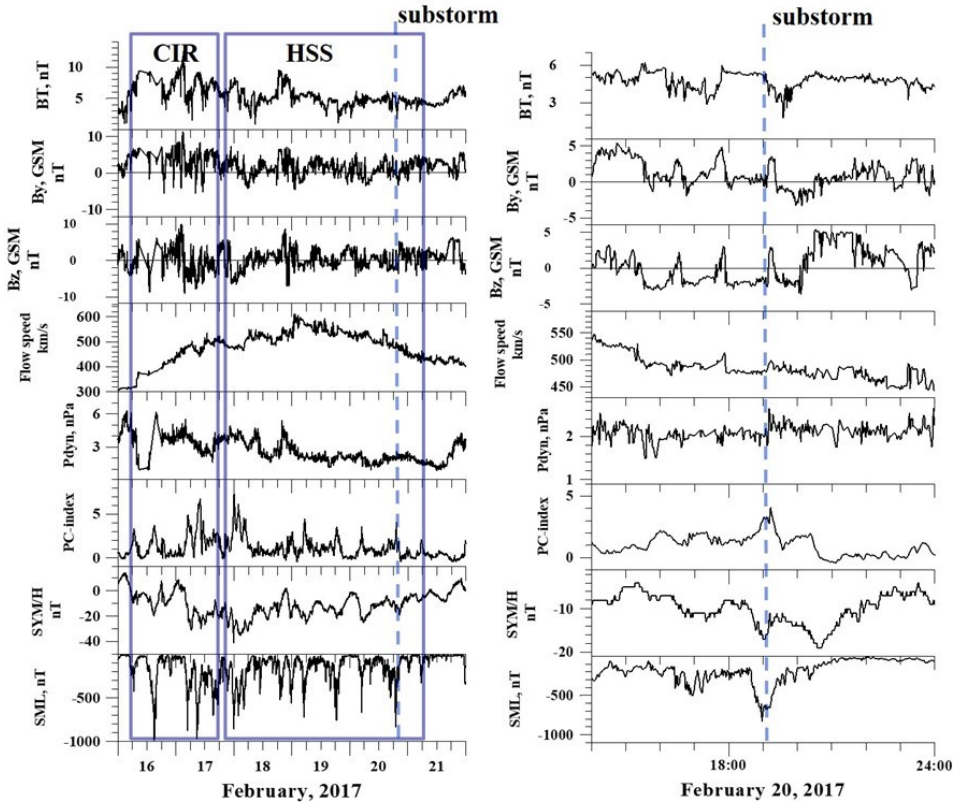

Fig.1. Solar wind and the interplanetary magnetic field components and some geomagnetic indices during the examined event on 20 February.

5. The substorm effect at midlatitudes

To study the substorm effects at midlatitudes, the spread region of the positive bays has been verified. The presence of positive bays at the IMAGE magnetometer network, in the longitudinal band 90°-105° GM longitude, at all European and a number of Asian and African stations has been ascertained. The latitudinal dependence of the positive bays amplitudes has been examined, the longitudinal and latitudinal extent of the positive bays and the central meridian of the substorm, have been estimated. Positive bays were observed at auroral, middle and even equatorial latitudes.

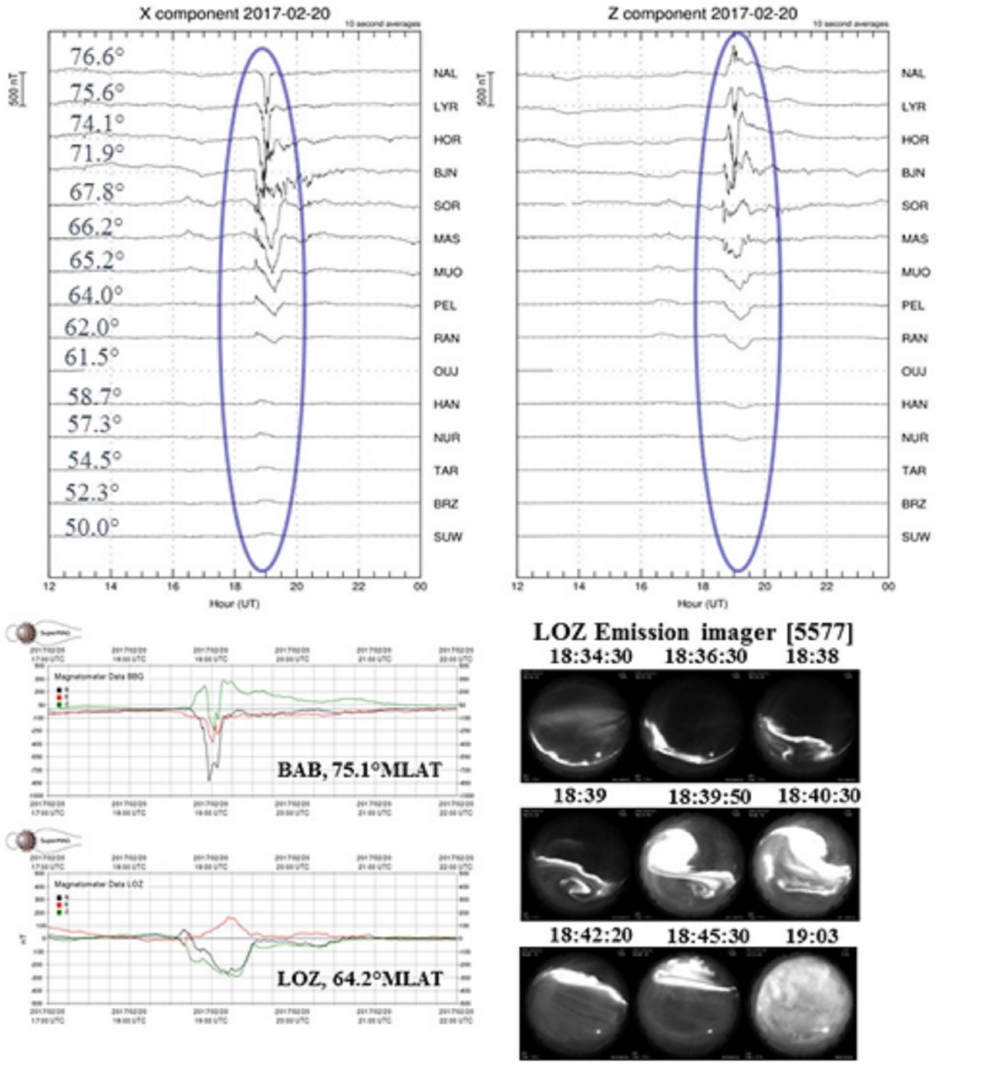

Fig.2. The development of the substorm at 18:40 UT on 20 February 2017 by IMAGE NAL-PPN chain X and Z magnetic components data (upper left and right panels, respectively), and by PGI data: magnetic field components at Barentsburg and Lovozero (left bottom panels) and 5577Å emission data at Lovozero (right bottom panel).

5.1. Positive bays by data of the IMAGE magnetometers network

The positive bays are observed at all IMAGE stations down from MEK (58.7°) and DOB (59.6°). In Fig.3 the X and Y components of all IMAGE stations with positive X bays (the two left panels) are presented, and the locations of these stations are shown (the right panel), indicated by stars.

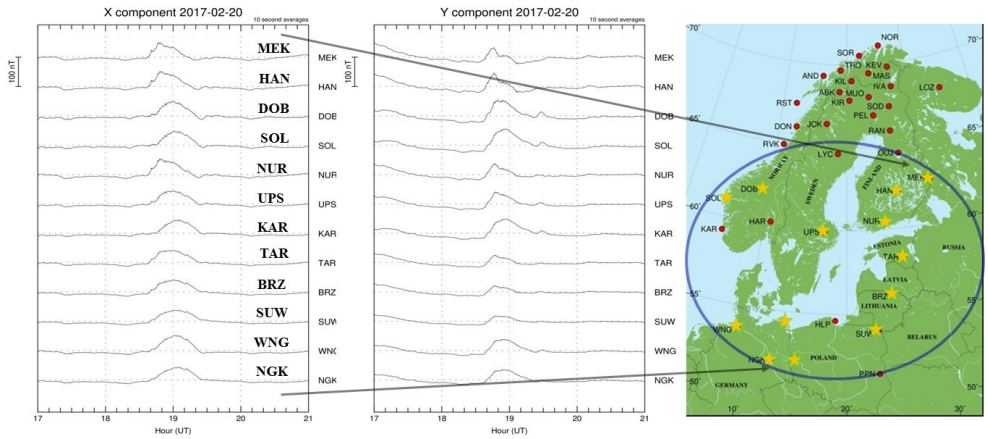

Fig.3. Two panels to the left: X and Y components of the magnetic field by all IMAGE stations where positive bays were observed. Right panel: locations of the IMAGE satations with positive X-bays, marked by stars.

5.2. MPB latitudinal dependance

To examine the MPB latitudinal dependence, data from the stations in the longitudinal band 90° - 104° GMLon, which is round the longitude of the Bulgarian station Panagjurishte (~97° GMLon) are used. In Fig.4, the X and Y components of chosen INTERMAGNET stations in this interval are shown. The substorm onset is marked by red vertical lines.

To build the MPB latitudinal dependence, stations data from the largest possible interval of geomagnetic latitudes with positive bays: 31.8° - 75.25° GMLat in the mensioned above longitudinal band were used. For the considered event on 20 February 2017, there were 20 stations with positive X bays in this area. The relationship between the MPB amplitude and the geomagnetic latitude is presented in Fig.5. The sign conversion latitude is marked by vertical line. Taking into account that there is a strong dependence on the geomagnetic longitude, as well, the longitudinal band was divided into three narrower strips (90°-95°, 95°-100°, 100°-105° GMLon). The data grouped in this way, are indicated by different symbols. It is seen, that the amplitude of the MPB decreases towards the lower latitudes.

5.3. Latitudinal extent of the positive bays

To determine with more precision the latitudinal extent of the MPB and the sign conversion latitude, the behaviour of the magnetic field components at more stations than the examined so far was verified, too. It was obtained that the highest latitude at which positive bays were registered, was 60.3° GMLat (HOV, Foroe Island station) (see Fig.6, left panel). Thus, 60° GMLat can be assumed as upper boundary of the latitudinal extent of MPB and the latitude of conversion of the bay sign. During the substorm positive bays were observed to equatorial stations as ABG (Alibag, 12° GMLat) and TAM (Tamanrasset, 8.9° GMLat) (shown in Fig.6, right panel). So, the latitudinal extent of the positive bays was ~51°.

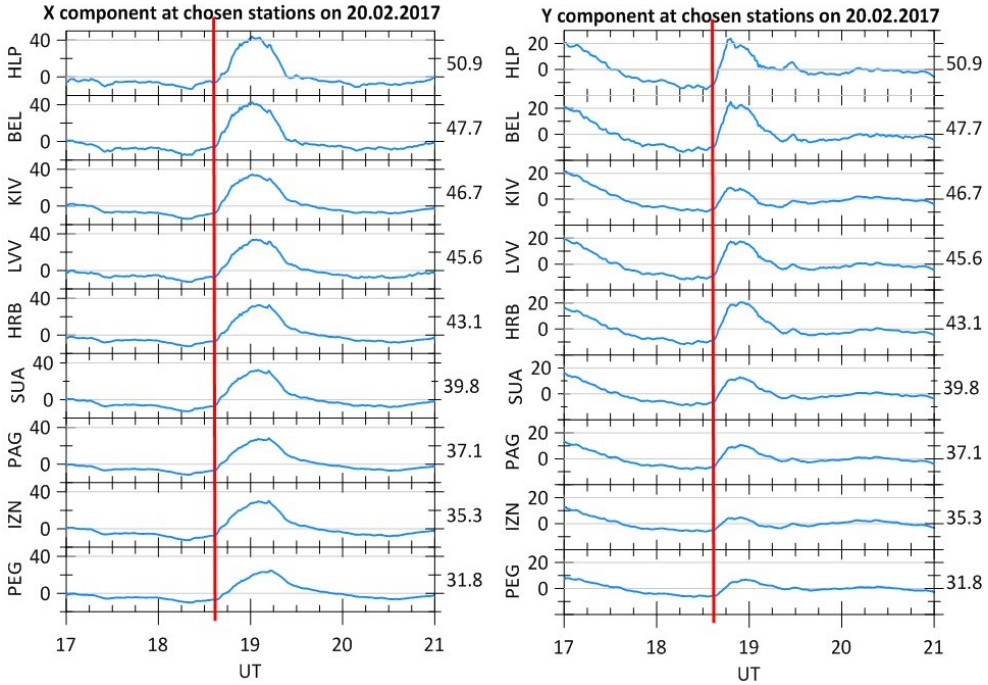

Fig.4. X (left panel) and Y (right panel) magnetic components at chosen INTERMAGNET stations from 17 UT to 21 UT on 20 February 2017.

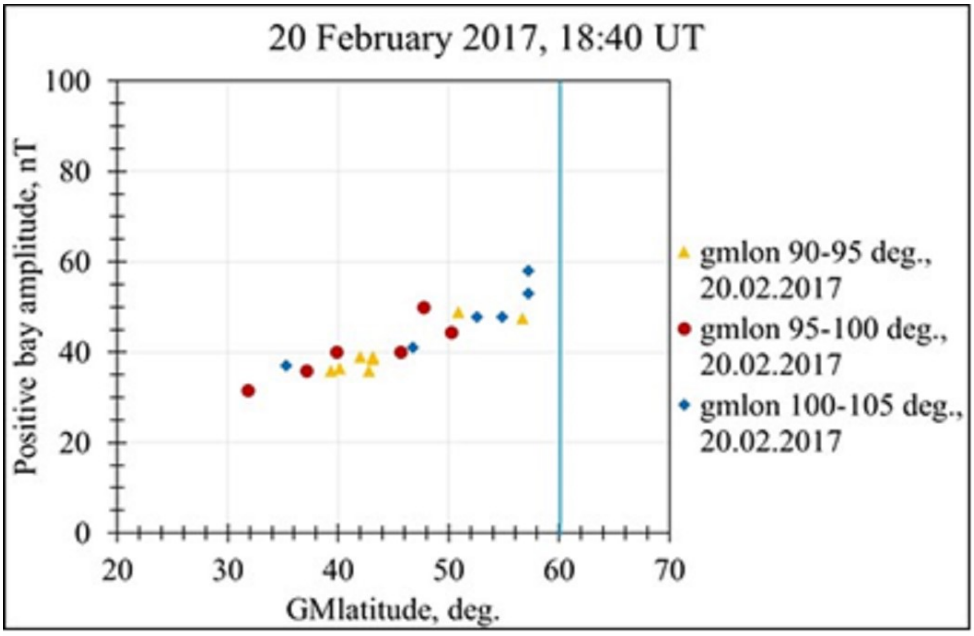

Fig.5. The dependence of magnetic positive bays (MPB) amplitude on the geomagnetic latitude for the substorms on 20 February 2017. The results for the examined longitudinal intervals are marked as follows: 90°-95° GMLon – by triangles, 95°-100° GMLon – by circles, and 100°-104° GMLon – by diamonds (shown in the right part of the panel).

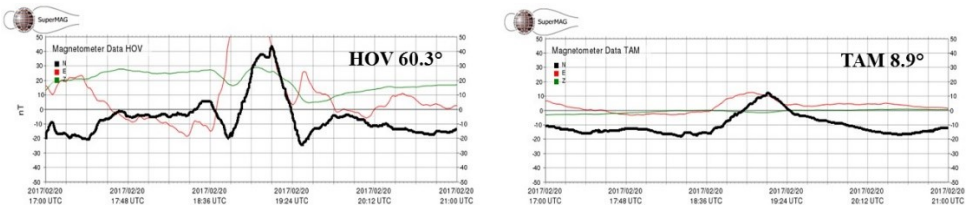

Fig.6. Midlatitude positive bays, observed at the highest geomagnetic latitude (HOV, Faroe Island station, 60.3° GMLat) (left panel) and at the lowest geomagnetic latitude (TAM, Tamanrasset, 8.9° GMLat) (right panel). The X component is drown by a thick line.

5.4. Estimation of the longitudinal extent of the positive bays

During the event on 20 February 2017, the positive bays were observed from ~70° GMLon to ~155° GMLon. In the left panel of Fig.7, the magnetic field components at the station with the most West location with registered positive bay, VAL (Valentia, Ireland, 70.3° GMLon) are shown. VAL is the most West European station. In the right panel, the magnetic components at the most East station with observed positive X-bay, NVS (Novosibirsk, Russia, 155.7° GMLon) is presented. So, the longitudinal extent of this substorm was ~85°.

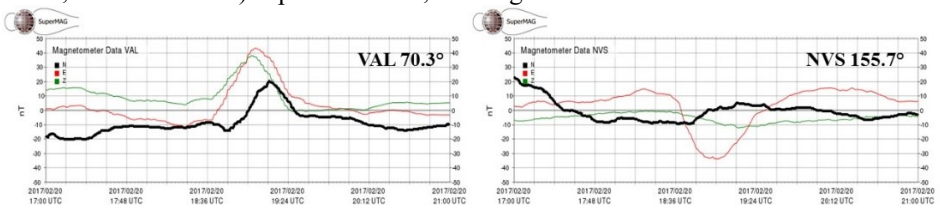

Fig.7. Records of the magnetic components at the most western (left panel) and most eastern (right panel) locations where MPB were observed. The X component is drown by thick line.

5.5. Determination of the central meridian of the substorm

It is known, that based on the peculiarities of the midlatitude positive bays a method to determine the geomagnetic longitude of the auroral substorm onset was worked out [21, 22]. It was established, that at middle latitudes, the azimuthal component of the magnetic field is positive to the West from the electrojet center, and negative – to the East from it. At the central meridian of the substorm the Y component passes through zero from positive to negative values.

The central meridian of the examined substorm was estimated by data of the IMAGE and SuperMag databases.

For the concidered event, positive Y values corresponded to the positive X bays of the IMAGE magnetometers network (see Fig.3, middle panel), hence, the IMAGE magnetometers were to the West from the center of the electrojet. In Fig.8 some examples of registered components to confirm the determination of the substorm central meridian are presented. The most eastern stations with positive sign of Y are MEK (Mekrijärvi, 59.1° GMLat, 108.5° GMLon), SPG (Saint Petersburg, 57.2° GMLat, 105.8° GMLon), MNK (Minsk, 50.8° GMLat, 103.3° GMLon), KIV (Kiev, 46.7° GMLat, 104.0° GMLon) and ODE (Odessa, 42.1° GMLat, 104.5° GMLon). So, the region of 103.3° - 108.5°, and of all latitudes below 59° GMLat was to the West from the center of the electrojet. As an example, the magnetic components at KIV are presented in the left upper panel of Fig.8.

The first station to the East of this region with negative Y component during the substorm, is KLI (Klimovskaya, 57.5° GMLat, 115.5° GMLon). Therfore this longitude was to the East of the central meridian of the substorm. The magnetic components at KLI are shown in the left bottom panel of Fig.8.

The change of the sign of the Y component was observed at the stations MOS (Moskow, 51.9° GMLat, 112.1° GMLon) and BOX (Borok, 54.6° GMLat, 114.2° GMLon). The registered magnetic components at these stations are presented in the middle panels of Fig.8. Thus, the central meridian of the substorm was located at about 112°-114° GMlon.It is indicated by a continuous line in the right panel of Fig.8, on the map of the magnetic vectors during the substorm by SuperMAG. The determined longitudinal boundaries of the substorm are indicated by dotted lines in the same panel.

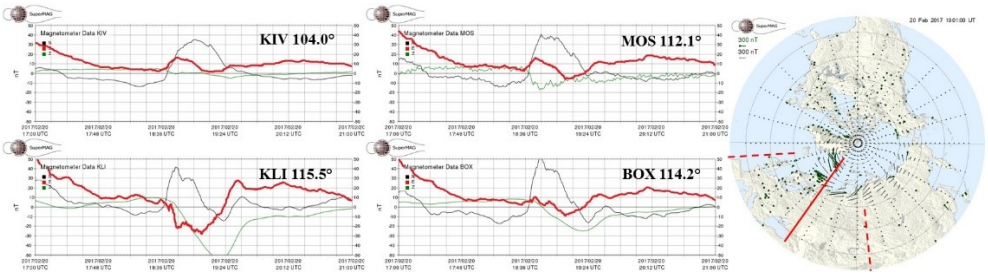

Fig.8. Examples of positive Y component (upper left panel), negative Y component (bottom left panel), and of cases, where Y passes through zero (middle panels). The Y component is marked by a thick line. The right panel presents the magnetic field vectors during the substorm (at 19:01 UT) by SuperMAG. The determined central meridian of the substorm is indicated by a continuous line, and the longitudinal boundaries of the positive bays extent – by dotted lines.

6. Discussion

We compaired some characteristics of the considered here substorm with our earlier results about the midlatitude effects of substorms.

The substrm, examined in [23], at 29:12 UT, on 27 September 2020, resemble to the studied here event. This substorm occurred also during HSS, in non-storm conditions, but just before the substorm, Sheath and Ejecta in the solar wind were observed. Thus, the interplanetary conditions were some more disturbed. The substorm on 27.09.2020 started at auroral latitudes, ~67° GMLat (SOR), and the center of the electrojet propagated to ~75° GMLat (HOR-LYR). The sign conversion latitude of the magnetic bays in this case was observed at lower latitudes, ~56° GMLat. Probably this is due to the more disturbed conditions in this case. Moreover, the conversion latitude during the other event, studied in [23] – the substorm at 21:25 UT on 6 February 2018, a usual substorm, generated during quiet conditions, when slow solar wind flow was observed, appeared at higher latitude, ~63° GMLat. In the study of usual and expanded subtorms during large geomagnetic storms the sign conversion latitude was observed in the range 50°-56° GMLat [24]. So, from these examples it follows, that the more disturbed are the interplanetary conditions, the more low is the conversion latitude of the substorms X magnetic bays.

The obtained dependence of the positive bays amplitudes has a similar shape, as the obtained in [23]: as a hole, it decreases with the latitude. A slight maximum at about 50° is observed here, as in the cases considered in [23]. The rise after the conversion latitude, obtained in [23], is not clearly expressed in the considered here substorm on 20 February 2017.

The mean amplitude of the positive bays during the substorm on 20 February 2017 was 42.4 nT, against the result of 55 nT for 27 September 2020 and 13.7 nT for 06 February 2018. The amplitudes of the positive bays during large geomagnetic storms were ~100-150 nT [24], and they were larger for the expanded substorm than for the usual ones. This result confirms, that the positive bays amplitude is greater in more disturbed conditions.

7. Summary

Expanded substorms are accompanied by midlatitude positive bays, the maximum amplitude of which is observed in the midnight sector. For the considered substorm the sign conversion latitude (~60°GMlat), the central meridian (~112°-114°GMlon), the latitudinal extent (~51°) and the longitudinal extent (~85°) of the positive bays were determined.

The observed conversion latitude for the examined substorm is typical for "expanded" substorms (~60° GMlat), it is higher than for the storm-time substorms or usual substorms.

For "expanded" substorms the amplitude of the bays is higher than for usual substorms. The amplitude of the positive bays as a whole, decreases with the latitude. A slight maximum at about 50° GM latitude is obtained.

A difference of about 50% between the minimal and maximal positive amplitude at different latitudes in the interval 30°-60° GMlat and 95°-105° GMlon was obtained.

More data about the midlatitude positive bays behaviour are needed to make statistical conclusions.

Acknowledgements. The authors are grateful to the creators of the databases OMNI (http://omniweb.gsfc.nasa.gov), SuperMAG (http://supermag.jhuapl.edu/), IMAGE (http://space.fmi.fi/image/), WDS at Kyoto (http://wdc.kugi.kyoto-u.ac.jp/index.html) and the solar wind large-scale phenomena catalog (http://www.iki.rssi.ru/omni/) for the opportunity to use them in this work.
This study was supported by the National Science Fund of Bulgaria (NSFB) (project number КП-06-Русия/15) and by the RFBR (project number 20-55-18003Болг_а).

References

1. S.-I. Akasofu, Space Sci. Rev. **113**, 1-40 (2004)
2. S.-I. Akasofu, Planet. Space Sci., **12(**4), 273–282 (1964)
3. M.I. Pudovkin, O.A. Troshichev, Planet. Space Sci., **20**, 1773-1779 (1972)
4. E. Nielsen, J. Bamber, Z.-S. Chen, A. Brekke, A. Egeland, J.S. Murphree, D. Venkatesan, W.I. Axford, Ann. Geophys. **6**(5), 559-572 (1988)
5. I.V. Despirak, , A.A. Lyubchich, H.K. Biernat, A.G. Yahnin, Geomagn. Aeron., **48**(3), 284–292 (2008)
6. Y.L. Feldstein, G.V. Starkov, Planet. Space Sci., **15**(2), 209–229 (1967)
7. E. Tanskanen, T.I. Pulkkinen, H.E.J. Koskinen, J.A. Slavin, J. Geophys. Res., **107(**A6), SMP 15-1 – SMP 15-11 (2002)
8. N.E. Turner, W.D. Cramer, S.K. Earles, B.A. Emery, J. Atmos. Sol. Terr. Phys., **71**, 1023–1031 (2009)
9. V. Guineva, I. Despirak, B. Kozelov, Sun and Geosphere, **11**(2), 125-130 (2016)
10. V. Guineva, I.V. Despirak, R. Werner, J. Atmos. Sol. Terr. Phys., **177**, 63-72 (2018)
11. A.T.Y. Lui, , S.-I. Akasofu, E.W. Hones, Jr., S.J. Bame, C.E. McIlwain, J. Geophys. Res., **81**(7), 1415–1419 (1976)

12. R.L. McPherron, C.T. Russell, M.G. Kivelson, P.J. Coleman, Jr., Radio Sci., **8**(11), 1059-1076 (1973)
13. Y. Kamide, S.-I. Akasofu, S.E. Deforest, J.L. Kisabeth, Planet. Space Sci., **23**(4), 579-584 (1975)
14. N.G. Kleimenova, E.E. Antonova, O.V. Kozyreva, L.M. Malysheva, T.A. Kornilova, I.A. Kornilov, Geomagn. Aeron., **52**(6), 746–754 (2012)
15. I.V. Despirak, A.A. Lubchich, N.G. Kleimenova, J. Atmos. Sol. Terr. Phys., **177**, 54-62 (2018)
16. R.L. McPherron, C.T. Russell, M. Aubry, J. Geophys. Res., **78**(16), 3131–3149 (1973)
17. S.-I. Akasofu, S. Chapman, C.-I. Meng, J. Atmos. Terr. Phys., **27**, 1275–1305 (1965)
18. C.-I. Meng, S.-I. Akasofu, J. Geophys. Res., **74**, 4035–4053 (1969)
19. R.L. McPherron, Planet. Space Sci., **20**(9), 1521-1539 (1972)
20. V. Guineva, I. Despirak, B. Kozelov, Aerospace Res. in Bulgaria, **26**, 145-154 (2014)
21. G. Rostoker, S.-I. Akasofu, J. Foster, R.A. Greenwald, Y. Camide, K. Kawasaki, A.T.Y. Lui, R.L. McPherron, C.T. Russell, J. Geophys. Res., **85**(A4), 1663-1668 (1980)
22. В.А. Сергеев, Н.А.Цыганенко, Магнитосфера Земли, М., 1980. 174 с.
23. V. Guineva, R. Werner, I. Despirak, R. Bojilova, L. Raykova, C. R. Acad. Bulg. Sci., **74**(8), 1185-1193 (2021)
24. V. Guineva, I. Despirak, N. Kleimenova, Aerospace Res. In Bulgaria, **31**, 27-39 (2019)